

Localized stem structures in quasi-resonant two-soliton solutions for the asymmetric Nizhnik-Novikov-Veselov system

Feng Yuan^a, Jiguang Rao^b, Jingsong He^{c,*}, Yi Cheng^d

^aCollege of Science, Nanjing University of Posts and Telecommunications, Nanjing, 210023, P. R. China

^bSchool of Mathematics and Statistics, Hubei University of Science and Technology, Xianning 437100, P. R. China

^cInstitute for Advanced Study, Shenzhen University, Shenzhen, 518060, P. R. China

^dSchool of Mathematical Sciences, USTC, Hefei, Anhui 230026, P. R. China

Abstract

Elastic collisions of solitons generally have a finite phase shift. When the phase shift has a finitely large value, the two vertices of the (2+1)-dimensional 2-soliton are significantly separated due to the phase shift, accompanied by the formation of a local structure connecting the two V-shaped solitons. We define this local structure as the stem structure. This study systematically investigates the localized stem structures between two solitons in the (2+1)-dimensional asymmetric Nizhnik-Novikov-Veselov system. These stem structures, arising from quasi-resonant collisions between the solitons, exhibit distinct features of spatial locality and temporal invariance. We explore two scenarios: one characterized by weakly quasi-resonant collisions (i.e. $a_{12} \approx 0$), and the other by strongly quasi-resonant collisions (i.e. $a_{12} \approx +\infty$). Through mathematical analysis, we extract comprehensive insights into the trajectories, amplitudes, and velocities of the soliton arms. Furthermore, we discuss the characteristics of the stem structures, including their length and extreme points. Our findings shed new light on the interaction between solitons in the (2+1)-dimensional asymmetric Nizhnik-Novikov-Veselov system.

Keywords: Localized stem structure; Asymptotic form; Quasi-resonant collision.

1. Introduction

Due to their extensive applications in physics and engineering, the theory and experimental researches of nonlinear waves are flourishing. The intricate evolution of nonlinear wave packets is described by numerous nonlinear partial differential equations (NPDEs). Over the past few decades, these equations have been well studied analytically and numerically. A plethora of methods emerged for analyzing and dissecting solutions to various NPDEs, including the Inverse scattering method [1, 2], the Darboux transformation[3–6], and the Hirota bilinear method [7–10]. These techniques empowered researchers to tackle NPDEs more effectively, boosting the discoveries of a large number of nonlinear wave solutions such as breather, lump, rogue wave, and their hybrid solutions.

Among these solutions, solitons are the first to be studied. In 1965, Zabusky and Kruskal published a groundbreaking paper introducing the concept of soliton numerically for the Korteweg-de Vries (KdV) equation [11]. Shortly after that, the n -soliton solutions of the KdV equation were successfully derived in 1974 analytically by using newly invented tool–inverse scattering method [12]. After that, the soliton solutions have been constructed in many integrable partial differential equations (see a early collection

*Corresponding author. E-mails: hejingsong@szu.edu.cn

in reference [13]). The potential of the soliton solutions in explaining natural phenomena is further explored and has been extended into various fields [14], such as plasma, nonlinear optics, Bose-Einstein condensation and many other fields.

The study of soliton interactions is a fundamental aspect of soliton theory. Solitons typically exhibit the following characteristics [11–15]:

- Solitons are spatially localized traveling wave solutions, maintaining a constant shape and velocity throughout their motion.
- If interactions between multiple solitons are elastic, after collision, the solitons regain their initial velocities with an extra phase shift. The phase of a soliton refers to the position of its wave crest, while phase shift denotes the variation in the soliton’s phase during transmission. This phase shift is primarily determined by the interplay between nonlinear effects and dispersive effects, maintaining constancy in both the time and frequency domains.
- Elastic collisions of two crossed solitons result in an X-shaped configuration, leading to their classification as X-shape solitons.

The elastic collisions display discernible finite phase shifts. Moreover, when the phase shift in an elastic collision approaches infinity, albeit remaining finite, it is termed a quasi-resonant collision. In recent years, heightened scholarly attention has been directed towards the investigation of high-dimensional soliton equations, particularly those in the (2+1)-dimensional framework. Ordinarily, two-dimensional line solitons propagate infinitely across space; however, notably, these collisions can engender localized stem structures. The concept of a stem structure originally pertains to the intermediary wave linking the incident and reflected waves in Mach reflection (see [16, 17]). Under the quasi-resonant state, the vertices of X-shaped solitons become substantially spaced apart due to phase delay, forming two V-shaped regions interconnected by a novel isolated wave, also referred to as a stem (see Ref. [18]). In this paper, we define the local structure that connects different soliton vertices, generated by the interaction between solitons, as the stem structure.

The stem structure of solitons has been discussed in previous studies, though the research is not extensive. For instance, Reference [19] examined the construction of quasi-resonant solitons within an extended Boussinesq-like equation. Reference [20] provided asymptotic forms of quasi-resonant two-solitons for the Kadomtsev-Petviashvili equation, wherein the stem structure is referred to as a virtual soliton. In 2012, Mark J. Ablowitz and Douglas E. Baldwin [21] reported quasi-resonant two-soliton water waves observed near low tide on two flat beaches located approximately 2000 km apart. However, only a few graphs (Fig. 3 and 4 in Ref. [21]) were presented, and the local characteristics of the intermediate wave (stem structure), such as its height, length and location, were not subjected to further analysis.

Considering the prevailing researches mainly focus on the solitons themselves and the scant detailed explorations on the attributes of the stem structure beyond preliminary analysis and intuitive graphical representation, we aim to investigate the localized stem structures within the (2+1)-dimensional asymmetric Nizhnik-Novikov-Veselov (ANNV) system through analytical methods and delve into their local properties.

The (2+1)-dimensional asymmetric Nizhnik-Novikov-Veselov (ANNV) system, first introduced by Boiti et al., is represented by the following form [22]:

$$\begin{cases} u_t + v_{xxx} = 3(uv)_x, \\ u_x = v_y. \end{cases} \quad (1)$$

Here, u and v represent the components of dimensionless velocity. The ANNV system (1) can explain various important physical phenomena such as the shallow waves driven by weakly nonlinear restoring

forces in incompressible fluids, the long internal waves within a density-stratified ocean, and the acoustic waves on a crystal lattice. The ANNV system extends the scope of the Hirota and Satsuma equation [23], making it a versatile framework for understanding diverse physical systems. Reference [22] proved that Eq. (1) can be simplified as the KdV equation when $x = y$ [22]. It can be also derived through the application of the inner parameter-dependent symmetry constraint of the KP equation [24]. Clarkson and Mansfield have explored several key aspects of the ANNV system, including the examination of the Painlevé property and the investigation of similarity solutions [25]. Additionally, various types of solutions have been reported, including dromion and kink solutions [26, 27], variable separation solutions [28], quasi-periodic solutions [29], soliton solutions [30], lump-type solutions [31–33] and rational and semi-rational solutions [34, 35].

Recently, resonance Y-shape soliton solutions of Eq. 1 have been formulated in Ref. [36, 37]. However, the X-shape solitons with constant length stems have not been constructed. The essential difficult problem in this study is to determine explicit expressions of the stem wave and its two ends. This leaves considerable room for understanding soliton interactions, which forms the primary focus of this paper. The basic purpose of us is to overcome unravelled problem in references [21, 36, 37] on the stem structure and then establish following objectives: (1) We construct constant length stem structure in two soliton solutions generated by quasi-resonant collisions. (2) We further propose two distinct ways of soliton construction, namely, via the weakly quasi-resonant collision when $a_{12} \approx 0$ and the strongly quasi-resonant collision when $a_{12} \approx +\infty$. (3) Meanwhile, we, for the first time, provide systematical exploration on the localization and dynamical characteristics of the stem structures.

The structure of the paper is organized as follows: In Sec. 2, we introduce the expressions of the Hirota Bilinear form and solutions of the ANNV system (1). In Sec. 3 and 4, we investigate the constant length stem structures in two soliton solutions generated by the weakly and strongly quasi-resonant collision, respectively. Their localization and dynamical properties are also provided. Finally, in Sec. 5, we summarize and discuss our results.

2. Basic formulas of Hirota Bilinear form and soliton solutions

In this section, we recall the Hirota Bilinear form and n -soliton solutions of the ANNV system (1). By using the transformation

$$u = -2(\ln f)_{xx}, \quad v = -2(\ln f)_{xy}, \quad (2)$$

it has the bilinear form[38]

$$D_y(D_t + D_x^3)f \cdot f = 0, \quad (3)$$

where D is defined by [7, 39]

$$D_t^m D_x^n D_y^r f(x, y, t) \cdot g(x, y, t) = \left(\frac{\partial}{\partial t} - \frac{\partial}{\partial t'}\right)^m \left(\frac{\partial}{\partial x} - \frac{\partial}{\partial x'}\right)^n \left(\frac{\partial}{\partial y} - \frac{\partial}{\partial y'}\right)^r f(x, y, t) g(x', y', t') \Big|_{x'=x, y'=y, t'=t},$$

and m, n, r are nonnegative integers. The N -soliton solutions of (1) have been given by the following form:

$$f^{[N]} = \sum_{\mu=0,1} \exp\left(\sum_{i<j}^N \mu_i \mu_j A_{ij} + \sum_{i=1}^N \mu_i \xi_i\right), \quad (4)$$

where,

$$\xi_j = k_j x + p_j y - k_j^3 t + \xi_j^0, \quad \exp(A_{ij}) = \frac{(k_i - k_j)(p_i - p_j)}{(k_i + k_j)(p_i + p_j)} \triangleq a_{ij} \geq 0. \quad (5)$$

Table 1: Physical quantities of the soliton arms

Soliton	Trajectory	Velocity	Amplitude	Components
S_j	l_j	$(k_j^2, -\frac{k_j}{p_j})$	$-\frac{k_j p_j}{2}$ $\frac{k_j^2}{2}$ $-\frac{j}{2}$	u_j v_j
S_j	\tilde{l}_j	$(k_j^2, -\frac{k_j}{p_j})$	$-\frac{k_j p_j}{2}$ $\frac{k_j^2}{2}$ $-\frac{j}{2}$	\tilde{u}_j \tilde{v}_j
S_{1-2}	l_{1-2}	$(k_1^2 + k_1 k_2 + k_2^2, -\frac{k_1^3 - k_2^3}{p_1 - p_2})$	$-\frac{(k_1 - k_2)(p_1 - p_2)}{2}$ $-\frac{(k_1 - k_2)^2}{2}$	u_{1-2} v_{1-2}

The j -th soliton S_j ($j = 1, 2, 1-2$) is composed by two components, u_j and v_j , and their key properties are summarized by Table 1. The relevant formulas are listed by (13).

The 1-soliton solution of Eq. (1) is $u^{[1]} = -\frac{k_1 p_1}{2} \operatorname{sech}^2(\frac{\xi_1}{2})$, $v^{[1]} = -\frac{k_1^2}{2} \operatorname{sech}^2(\frac{\xi_1}{2})$. It's readily to know that both $u^{[1]}$ and $v^{[1]}$ have trajectories of $\xi_1 = 0$, while their amplitudes are $u_{amp} = -\frac{k_1 p_1}{2}$ and $v_{amp} = -\frac{k_1^2}{2}$, respectively. Then it can be seen that $u^{[1]}$ is a dark soliton when $k_1 p_1 > 0$ and it is a bright soliton when $k_1 p_1 < 0$, while $v^{[1]}$ is always a dark soliton.

In this paper, we focus on the 2-soliton solution of the ANNV system. Substituting $N = 2$ into Eq. (4), the fundamental 2-soliton solution can be obtained by (2) and the following equation,

$$f^{[2]} = 1 + e^{\xi_1} + e^{\xi_2} + a_{12} e^{\xi_1 + \xi_2}. \quad (6)$$

The phase shift of the 2-soliton solution is denoted as $\Delta_{12} = \ln a_{12}$. Different conditions on the phase shift give rise to distinct types of collisions between the two solitons, such as elastic collisions and resonance collisions. In the context of elastic collisions, a 2-soliton is X-shaped. When the phase shift is sufficiently large but finite, the two vertices of the X-shaped soliton are significantly separated due to this phase shift, forming a local structure that connects the two V-shaped solitons. Since 2-solitons are traveling waves, the stem structure also maintains its shape during propagation, resulting in a constant-length stem structure. The constant-length stem structure in quasi-resonant 2-solitons is the primary focus of our investigation. Subsequently, we will delve into the analysis of the localized stem structure under the condition $\Delta_{12} \approx \infty$, corresponding to either $a_{12} \approx 0$ or $a_{12} \approx +\infty$. We will explore these two cases in detail.

Remark 1. *The distinction between strongly and weakly resonances lies in their outcomes: a strongly resonance ($a_{ij} = +\infty$) between S_i ($f_i = 1 + \exp(\xi_i)$) and S_j ($f_j = 1 + \exp(\xi_j)$) produces a soliton S_{i+j} ($f_{i+j} = 1 + \exp(\xi_i + \xi_j)$), whereas a weakly resonance ($a_{ij} = 0$) yields S_{i-j} ($f_{i+j} = 1 + \exp(\xi_i - \xi_j)$). Similarly, we refer to strongly quasi-resonance when $a_{ij} \approx +\infty$ and weakly quasi-resonance when $a_{ij} \approx 0$.*

3. Constant length stem structure generated by weakly quasi-resonant collision

In the scenario where $a_{12} \approx 0$ ($\Delta_{12} \approx -\infty$), we initially examine the asymptotic properties of the 2-soliton by the asymptotic analysis method given in Ref. [19, 20, 40]. To analyze the asymptotic behavior of the soliton S_1 , we express the tau function (6) as:

$$f = 1 + e^{\xi_1} + e^{\xi_2} (1 + e^{\xi_1 + \ln a_{12}}). \quad (7)$$

For $\xi_1 \approx 0$, $\xi_2 \rightarrow -\infty$, Eq. (7) can be approximated by

$$f \approx f_1 = 1 + e^{\xi_1}.$$

Similarly, for $\xi_1 + \ln a_{12} \approx 0$, $\xi_2 \rightarrow +\infty$, Eq. (7) can be approximated by

$$f \approx \widetilde{f}_1 = 1 + a_{12}e^{\xi_1}.$$

The asymptotic properties of soliton S_2 are studied in a similar manner, with the tau function (6) expressed by

$$f = 1 + e^{\xi_2} + e^{\xi_1}(1 + e^{\xi_2 + \ln a_{12}}). \quad (8)$$

For $\xi_2 \approx 0$, $\xi_1 \rightarrow -\infty$, Eq. (8) can be approximated by

$$f \approx f_2 = 1 + e^{\xi_2}.$$

For $\xi_2 + \ln a_{12} \approx 0$, $\xi_1 \rightarrow +\infty$, Eq. (7) can be approximated by

$$f \approx \widetilde{f}_2 = 1 + a_{12}e^{\xi_2}.$$

Finally, we examine the asymptotic properties of the constant length stem. In the case of $\xi_1 \approx \xi_2$, $\xi_{1,2} \rightarrow +\infty$, and $a_{12} \approx 0$, we observe that $e^{\xi_1} + e^{\xi_2}$ is much larger than $1 + a_{12}e^{\xi_1 + \xi_2}$. Consequently, Eq. (8) can be approximated as:

$$f \approx f_{1-2} = e^{\xi_1} + e^{\xi_2} = e^{\xi_2}(1 + e^{\xi_1 - \xi_2}).$$

Based on the above asymptotic analysis, the 2-soliton undergoes weakly quasi-resonant collisions, as manifested in the following asymptotic forms:

Before collision:

$$\begin{aligned} \text{The soliton } S_1 (\xi_1 \approx 0, \xi_2 \rightarrow -\infty) : u &\approx u_1, v \approx v_1, \\ \text{The soliton } S_2 (\xi_2 + \ln a_{12} \approx 0, \xi_1 \rightarrow +\infty) : u &\approx \widetilde{u}_2, v \approx \widetilde{v}_2, \end{aligned} \quad (9)$$

After collision:

$$\begin{aligned} \text{The soliton } S_1 (\xi_1 + \ln a_{12} \approx 0, \xi_2 \rightarrow +\infty) : u &\approx \widetilde{u}_1, v \approx \widetilde{v}_1, \\ \text{The soliton } S_2 (\xi_2 \approx 0, \xi_1 \rightarrow -\infty) : u &\approx u_2, v \approx v_2; \end{aligned} \quad (10)$$

The constant length stem:

$$\text{The soliton } S_{1-2} (\xi_1 \approx \xi_2, \xi_{1,2} \rightarrow +\infty) : u \approx u_{1-2}, v \approx v_{1-2}. \quad (11)$$

Here, the formulas of the soliton arms in (9)–(11) are given as following,

$$\begin{aligned} u_j &= -\frac{k_j p_j}{2} \operatorname{sech}^2\left(\frac{\xi_j}{2}\right), v_j = -\frac{k_j^2}{2} \operatorname{sech}^2\left(\frac{\xi_j}{2}\right), j = 1, 2, \\ \widetilde{u}_j &= -\frac{k_j p_j}{2} \operatorname{sech}^2\left(\frac{\xi_j + \ln a_{12}}{2}\right), \widetilde{v}_j = -\frac{k_j^2}{2} \operatorname{sech}^2\left(\frac{\xi_j + \ln a_{12}}{2}\right), \\ u_{1-2} &= -\frac{(k_1 - k_2)(p_1 - p_2)}{2} \operatorname{sech}^2\left(\frac{\xi_1 - \xi_2}{2}\right), v_{1-2} = -\frac{(k_1 - k_2)^2}{2} \operatorname{sech}^2\left(\frac{\xi_1 - \xi_2}{2}\right). \end{aligned} \quad (12)$$

The stem S_{1-2} is also denoted as a virtual soliton and was initially introduced in reference [19] for the extended Boussinesq-like equation, and subsequently in reference [20] for the Kadomtsev-Petviashvili equation. These structures have been depicted graphically. It is noteworthy that the localized characteristics of the stem structures, including trajectory and endpoint coordinates, have not been rigorously analyzed. Consequently, our attention now shifts towards the analytical study concerning the stem structure.

Undoubtedly, this soliton exhibits five arms. Table 1 provides the formulas, trajectories, amplitudes, and velocities for each arm, while the pertinent formulae are given by (12) and

$$l_1: \xi_1 = 0, \quad l_2: \xi_2 = 0, \quad \tilde{l}_1: \xi_1 + \ln a_{12} = 0, \quad \tilde{l}_2: \xi_2 + \ln a_{12} = 0, \quad l_{1-2}: \xi_1 - \xi_2 = 0. \quad (13)$$

Solving a group of equations $\xi_1 = 0$ and $\xi_2 = 0$ implies an intersection point A on (x, y) -plane of l_1 and l_2 as:

$$A \left(\frac{(k_1^3 p_2 - k_2^3 p_1)t + p_1 \xi_2^0 - p_2 \xi_1^0}{k_1 p_2 - k_2 p_1}, -\frac{(k_1^3 k_2 - k_1 k_2^3)t + k_1 \xi_2^0 - k_2 \xi_1^0}{k_1 p_2 - k_2 p_1} \right). \quad (14)$$

Similarly, the intersection point B on (x, y) -plan of \tilde{l}_1 and \tilde{l}_2 can be generated as

$$B \left(\frac{(p_1 - p_2) \ln a_{12} + (k_1^3 p_2 - k_2^3 p_1)t + p_1 \xi_2^0 - p_2 \xi_1^0}{k_1 p_2 - k_2 p_1}, -\frac{(k_1 - k_2) \ln a_{12} + (k_1^3 k_2 - k_1 k_2^3)t + k_1 \xi_2^0 - k_2 \xi_1^0}{k_1 p_2 - k_2 p_1} \right), \quad (15)$$

by solving a group of $\xi_1 + \ln a_{12} = 0$ and $\xi_2 + \ln a_{12} = 0$. It is noteworthy that points A and B also serve as the endpoints of l_{1-2} , which can be seen in Fig. 1. Consequently, the length of the stem, denoted as $|AB|$, is defined as:

$$|AB| = \left| \frac{\ln a_{12}}{k_1 p_2 - k_2 p_1} \right| \sqrt{(k_1 - k_2)^2 + (p_1 - p_2)^2}. \quad (16)$$

This formula show that the length of the stem is constant. To ensure $a_{12} \approx 0$, it is imperative to set $k_1 \approx k_2$ or $p_1 \approx p_2$. Specifically, if $k_1 \approx k_2$, the stem's amplitude is almost zero. Consequently, the segment between A and B in Fig. 1 merges with the background plane. However, it is crucial to recognize that this segment comprises solitons of exceptionally small amplitude, as depicted in Fig. 1 (a) and (b). Notably, when $p_1 p_2 < 0$, u manifests as a dark-bright soliton, while $p_1 > 0$ and $p_2 > 0$ make u a 2-bright soliton. Conversely, if $p_1 \approx p_2$, the amplitude of the stem u_{1-2} nearly vanishes, while v_{1-2} remains non-zero, as illustrated in Fig. 1 (c) and (d). In this scenario, $k_1 > 0$ and $k_2 > 0$ make u a 2-dark soliton, whereas $k_1 k_2 < 0$ results in u being a dark-bright soliton.

Next, we explore the cross-sectional curves of the 2-soliton (2) on the planes $\xi_1 - \xi_2 = 0$:

When $k_1 \approx k_2$,

$$\begin{aligned} u|_{l_{1-2}}^{(1)} &= -\frac{2(k_1 p_1 + k_2 p_2)g_1 g_2 e^{3\theta_1} + 4g_1^2 g_2 e^{2\theta_1} + 2(k_1 p_1 + k_2 p_2)g_1^2 e^{\theta_1}}{(g_2 e^{2\theta_1} + 2g_1 e^{\theta_1} + g_1)^2}; \\ v|_{l_{1-2}}^{(1)} &= -\frac{2(k_1^2 + k_2^2)g_1 g_2 e^{3\theta_1} + 4(k_1 p_1 - k_2 p_2)(k_1^2 - k_2^2)g_1 e^{2\theta_1} + 2g_1^2(k_1^2 + k_2^2)e^{\theta_1}}{(g_2 e^{2\theta_1} + 2g_1 e^{\theta_1} + g_1)^2}; \end{aligned} \quad (17)$$

When $p_1 \approx p_2$,

$$\begin{aligned} u|_{l_{1-2}}^{(2)} &= -\frac{2(k_1 p_1 + k_2 p_2)g_1 g_2 e^{3\theta_2} + 4g_1^2 g_2 e^{2\theta_2} + 2(k_1 p_1 + k_2 p_2)g_1^2 e^{\theta_2}}{(g_2 e^{2\theta_2} + 2g_1 e^{\theta_2} + g_1)^2}; \\ v|_{l_{1-2}}^{(2)} &= -\frac{2(k_1^2 + k_2^2)g_1 g_2 e^{3\theta_2} + 4(k_1 p_1 - k_2 p_2)(k_1^2 - k_2^2)g_1 e^{2\theta_2} + 2g_1^2(k_1^2 + k_2^2)e^{\theta_2}}{(g_2 e^{2\theta_2} + 2g_1 e^{\theta_2} + g_1)^2}; \end{aligned} \quad (18)$$

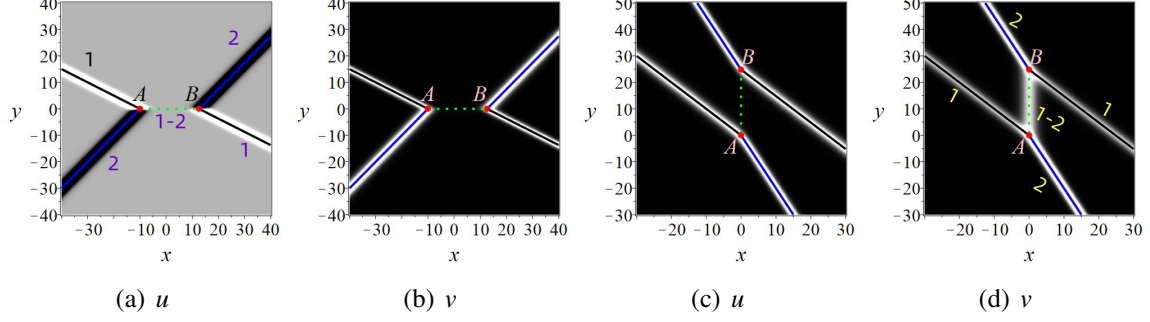


Figure 1: The density plots of the quasi-resonant two soliton with constant length stem structure. Parameters: (a) (b) $k_1 = 1$, $k_2 = 1 - 10^{-10}$, $p_1 = 2$, $p_2 = -1$, $\xi_1^0 = 10$, $\xi_2^0 = 10$, $t = 0$. (c) (d) $k_1 = 1$, $k_2 = 2$, $p_1 = 1$, $p_2 = 1 + 10^{-10}$, $\xi_1^0 = 0$, $\xi_2^0 = 0$, $t = 0$. The lines are the trajectories of S_j , and the red points are the endpoints of the stem which are expressed as Eqs. (14) and (15).

Here,

$$\theta_1 = \frac{p_1(k_2x - k_2^3t + \xi_2^0) - p_2(k_1x - k_1^3t + \xi_1^0)}{p_1 - p_2}, \quad \theta_2 = \frac{k_1(p_2y - k_2^3t + \xi_2^0) - k_2(p_1y - k_1^3t + \xi_1^0)}{k_1 - k_2}, \quad (19)$$

$$g_1 = (p_1 + p_2)(k_1 + k_2), \quad g_2 = (p_1 - p_2)(k_1 - k_2).$$

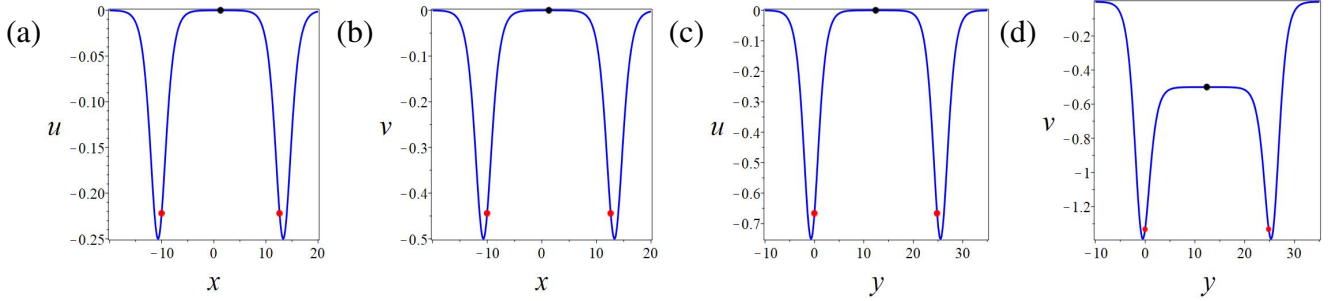


Figure 2: (a) (b) The cross-sectional curves (17) with parameters: $k_1 = 1$, $k_2 = 1 - 10^{-10}$, $p_1 = 2$, $p_2 = -1$; The black points are corresponding to P_1 , and the red points are corresponding to A and B . (c) (d) The cross-sectional curves (18) with parameters: $k_1 = 1$, $k_2 = 2$, $p_1 = 1$, $p_2 = 1 + 10^{-10}$.

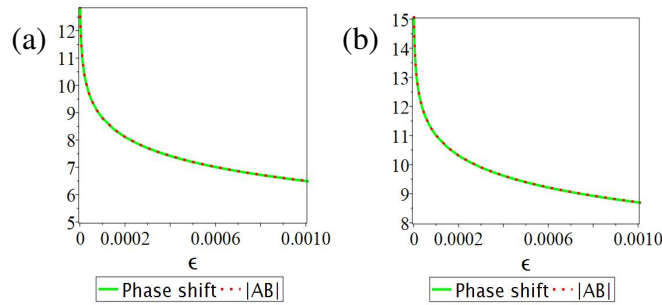


Figure 3: Parameters: (a) $k_1 = 1$, $k_2 = 1 - \epsilon$, $p_1 = 2$, $p_2 = -1$; (b) $k_1 = 1$, $k_2 = 2$, $p_1 = 1$, $p_2 = 1 + \epsilon$.

In general, the stem has a flat top on (or lower than) (x, y) -plane with two deep downward peaks, as verified in Fig. 2 illustrating the cross-sectional curves corresponding to Fig. 1. Deriving the extreme values by taking the derivative of Eq. (17), we observe that instead of a line soliton having an extreme

value line, the constant length stem S_{1-2} possesses only one extreme point between A and B . The extreme points of $u|_{l_{1-2}}^{(1)}$ and $v|_{l_{1-2}}^{(1)}$ share the same coordinates on the (x, y) -direction, as follows:

$$P_1 : \left(\frac{(p_1 - p_2) \ln a_{12} - 2p_1(k_2^3 t - \xi_2^0) + 2p_2(k_1^3 t - \xi_1^0)}{2(k_1 p_2 - k_2 p_1)}, -\frac{(k_1 - k_2) \ln a_{12} - 2k_1(k_2^3 t - \xi_2^0) + 2k_2(k_1^3 t - \xi_1^0)}{2(k_1 p_2 - k_2 p_1)} \right) \quad (20)$$

Remark 2. Since 2-soliton propagates within the (x, y) -plane, the point P_1 (the midpoint of the stem structure) also traverses the (x, y) -plane. Consequently, the coordinates of P_1 are functions of time t . This behavior similarly applies to the point P_2 (as described in Eq. (31) in Section 4).

It is noteworthy that P_1 precisely corresponds to the midpoint of AB , represented by black dots in Fig. 2. Substituting (20) into (2) and (6), we obtain the extreme values of S_{1-2} as $u(P_1) = -\frac{(k_1 - k_2)(p_1 - p_2)}{2\sqrt{a_{12}}} \approx -\frac{(k_1 - k_2)(p_1 - p_2)}{2}$ and $v(P_1) = -\frac{(k_1 - k_2)^2}{2} \cdot \frac{(k_1 + k_2)^2 \sqrt{a_{12} + (k_1 - k_2)^2}}{(k_1 - k_2)^2 (\sqrt{a_{12} + 1})} \approx -\frac{(k_1 - k_2)^2}{2}$. These approximations further validate the accuracy of the asymptotic forms (11). We can see from Fig. 2 that the two ends of the stem are not the maximum or minimum points of u or v .

Setting $|k_1 - k_2| = \epsilon \approx 0$ or $|p_1 - p_2| = \epsilon \approx 0$ with $|k_j|, |p_j| \gg \epsilon$, we find $|AB| \approx |\Delta_{12}|$. Figure 3 depict how “ $|AB|$ ” and “ $|\Delta_{12}|$ ” change concerning “ ϵ ”. It is evident that as $\epsilon \approx 0$, the “ $|AB|$ ” curve closely aligns with the phase curve, and a smaller ϵ corresponds to a longer stem.

4. Constant length stem structure generated by strongly quasi-resonant collision

In situations where $a_{12} \approx \infty$, ($\Delta_{12} \approx +\infty$), the 2-soliton undergoes strongly quasi-resonant collisions. The asymptotical properties of the soliton S_1 and S_2 are the same as the case $a_{12} \approx 0$, but the asymptotical properties of the stem are different. In the case of $\xi_1 \approx -\xi_2$, $\xi_1 \rightarrow +\infty$, $\xi_2 \rightarrow -\infty$, and $a_{12} \approx +\infty$, we observe that $1 + a_{12}e^{\xi_1 + \xi_2}$ is much larger than $e^{\xi_1} + e^{\xi_2}$. Consequently, Eq. (8) can be approximated as:

$$f \approx \widetilde{f}_{1+2} = 1 + a_{12}e^{\xi_1 + \xi_2}.$$

Based on the asymptotic analysis of S_1 , S_2 , and S_{1+2} , the 2-soliton experiences strongly elastic quasi-resonant manifests in the following asymptotic forms:

Before collision:

$$\begin{aligned} \text{The soliton } S_1 (\xi_1 \approx 0, \xi_2 \rightarrow -\infty) : u \approx u_1, v \approx v_1, \\ \text{The soliton } S_2 (\xi_2 + \ln a_{12} \approx 0, \xi_1 \rightarrow +\infty) : u \approx \widetilde{u}_2, v \approx \widetilde{v}_2; \end{aligned} \quad (21)$$

After collision:

$$\begin{aligned} \text{The soliton } S_1 (\xi_1 + \ln a_{12} \approx 0, \xi_2 \rightarrow +\infty) : u \approx \widetilde{u}_1, v \approx \widetilde{v}_1, \\ \text{The soliton } S_2 (\xi_2 \approx 0, \xi_1 \rightarrow -\infty) : u \approx u_2, v \approx v_2; \end{aligned} \quad (22)$$

The constant length stem:

$$\text{The soliton } S_{1+2} (\xi_1 \approx -\xi_2, \xi_1 \rightarrow +\infty, \xi_2 \rightarrow -\infty) : u \approx \widetilde{u}_{1+2}, v \approx \widetilde{v}_{1+2}. \quad (23)$$

The relevant expressions are provided in Eq. (12) and

$$\widetilde{u}_{1+2} = -\frac{(k_1 + k_2)(p_1 + p_2)}{2} \operatorname{sech}^2\left(\frac{\xi_1 + \xi_2 + \ln a_{12}}{2}\right), \quad \widetilde{v}_{1+2} = -\frac{(k_1 + k_2)^2}{2} \operatorname{sech}^2\left(\frac{\xi_1 + \xi_2 + \ln a_{12}}{2}\right). \quad (24)$$

Table 2: Physical quantities of the stem structures

Stem	Trajectory	Velocity	Amplitude	Components
S_{1+2}	\widetilde{l}_{1+2}	$(k_1^2 - k_1 k_2 + k_2^2, -\frac{k_1^3 + k_2^3}{p_1 + p_2})$	$-\frac{(k_1 + k_2)(p_1 + p_2)}{2}$ $-\frac{(k_1 + k_2)^2}{2}$	\widetilde{u}_{1+2} \widetilde{v}_{1+2}

The solitons S_{1+2} is composed by two components $u_{1\pm 2}$ and $v_{1\pm 2}$, and their trajectories are listed by (25).

This soliton also has five arms. The formulas, trajectories, amplitudes, velocities of these five arms before and after collision are provided in tables 1 and 2, while the pertinent formulae are given by (13) and following formula,

$$\widetilde{l}_{1+2}: \xi_1 + \xi_2 + \ln a_{12} = 0. \quad (25)$$

Solving the system of equations $\xi_1 = 0$ and $\xi_2 + \ln a_{12} = 0$ leads to an intersection point C on the (x, y) -plane of l_1 and \widetilde{l}_2 :

$$C \left(\frac{p_1 \ln a_{12} + (k_1^3 p_2 - k_2^3 p_1)t + p_1 \xi_2^0 - p_2 \xi_1^0}{k_1 p_2 - k_2 p_1}, -\frac{k_1 \ln a_{12} + (k_1^3 k_2 - k_1 k_2^3)t + k_1 \xi_2^0 - k_2 \xi_1^0}{k_1 p_2 - k_2 p_1} \right). \quad (26)$$

Similarly, solving the system $\xi_1 + \ln a_{12} = 0$ and $\xi_2 = 0$ yields an intersection point D on the (x, y) -plane of l_2 and \widetilde{l}_1 :

$$D \left(\frac{-p_2 \ln a_{12} + (k_1^3 p_2 - k_2^3 p_1)t + p_1 \xi_2^0 - p_2 \xi_1^0}{k_1 p_2 - k_2 p_1}, -\frac{-k_2 \ln a_{12} + (k_1^3 k_2 - k_1 k_2^3)t + k_1 \xi_2^0 - k_2 \xi_1^0}{k_1 p_2 - k_2 p_1} \right). \quad (27)$$

Then we can also obtain the length of the constant length stem as

$$|CD| = \left| \frac{\ln a_{12}}{k_1 p_2 - k_2 p_1} \right| \sqrt{(k_1 + k_2)^2 + (p_1 + p_2)^2}. \quad (28)$$

To ensure that $a_{12} \approx \infty$, it is necessary to set either $k_1 \approx -k_2$ or $p_1 \approx -p_2$. When $k_1 \approx -k_2$, the table 2 reveals that the amplitude of the stem \widetilde{S}_{1+2} approaches zero, as illustrated in Fig. 4 (a) and (b). Alternatively, if $p_1 \approx -p_2$, the amplitude of \widetilde{u}_{1+2} is almost zero, while \widetilde{v}_{1+2} does not, as depicted in Fig. 4 (c) and (d). Subsequently, an investigation of the 2-soliton (2) is conducted on the cross-sectional curves situated on planes defined by $\xi_1 + \xi_2 + \ln a_{12} = 0$, formulated as follows:

When $k_1 \approx -k_2$,

$$\begin{aligned} u|_{\widetilde{l}_{1+2}}^{(1)} &= -\frac{2(k_1 p_1 + k_2 p_2)(e^{\theta_3} + e^{\theta_4}) + 4g_1}{(e^{\theta_3} + e^{\theta_4} + 2)^2}; \\ v|_{\widetilde{l}_{1+2}}^{(1)} &= -\frac{2(k_1^2 + k_2^2)(p_1 - p_2)(e^{\theta_3} + e^{\theta_4}) + 4(k_1 + k_2)(k_1 p_1 + k_2 p_2)}{(p_1 - p_2)(e^{\theta_3} + e^{\theta_4} + 2)^2}; \end{aligned} \quad (29)$$

When $p_1 \approx -p_2$,

$$\begin{aligned} u|_{\widetilde{l}_{1+2}}^{(2)} &= -\frac{2(k_1 p_1 + k_2 p_2)(e^{\theta_5} + e^{\theta_6}) + 4g_1}{(e^{\theta_5} + e^{\theta_6} + 2)^2}; \\ v|_{\widetilde{l}_{1+2}}^{(2)} &= -\frac{2(k_1^2 + k_2^2)(p_1 - p_2)(e^{\theta_5} + e^{\theta_6}) + 4(k_1 + k_2)(k_1 p_1 + k_2 p_2)}{(p_1 - p_2)(e^{\theta_5} + e^{\theta_6} + 2)^2}; \end{aligned} \quad (30)$$

Here, g_1, g_2 are given in (19) and

$$\theta_3 = \frac{p_1(k_2x - k_2^3t + \xi_2^0) - p_2(k_1x - k_1^3t + \xi_1^0 + \ln a_{12})}{p_1 + p_2}, \theta_4 = \frac{-p_1(k_2x - k_2^3t + \xi_2^0 + \ln a_{12}) + p_2(k_1x - k_1^3t + \xi_1^0)}{p_1 + p_2},$$

$$\theta_5 = \frac{k_1(p_2y - k_2^3t + \xi_2^0) - k_2(p_1y - k_1^3t + \xi_1^0 + \ln a_{12})}{k_1 + k_2}, \theta_6 = \frac{-k_1(p_2y - k_2^3t + \xi_2^0 + \ln a_{12}) + k_2(p_1y - k_1^3t + \xi_1^0)}{k_1 + k_2}.$$

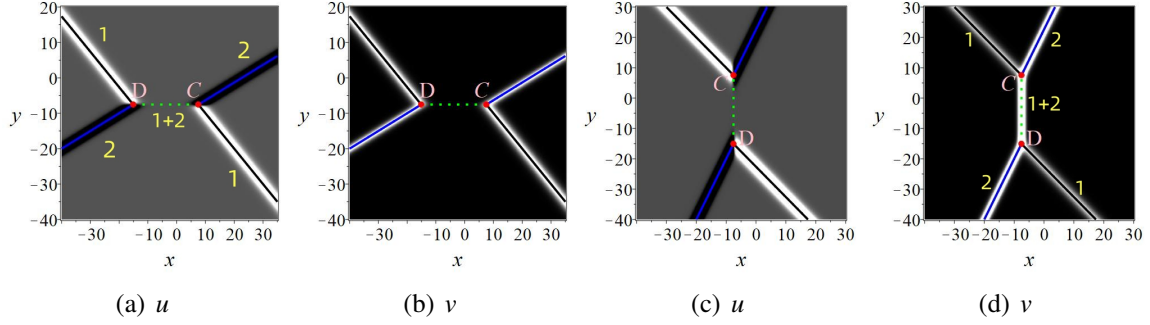


Figure 4: The density plots of the quasi-resonant two soliton with constant length stem structure. Parameters: (a) (b) $k_1 = 1, k_2 = -1 - 10^{-10}, p_1 = 1, p_2 = 2, \xi_1^0 = 0, \xi_2^0 = 0, t = 0$. (c) (d) $k_1 = 1, k_2 = 2, p_1 = 1, p_2 = -1 - 10^{-10}, \xi_1^0 = 0, \xi_2^0 = 0, t = 0$. The lines are the trajectories of S_j , and the red points are the endpoints of the stem which are expressed as Eqs. (26) and (27).

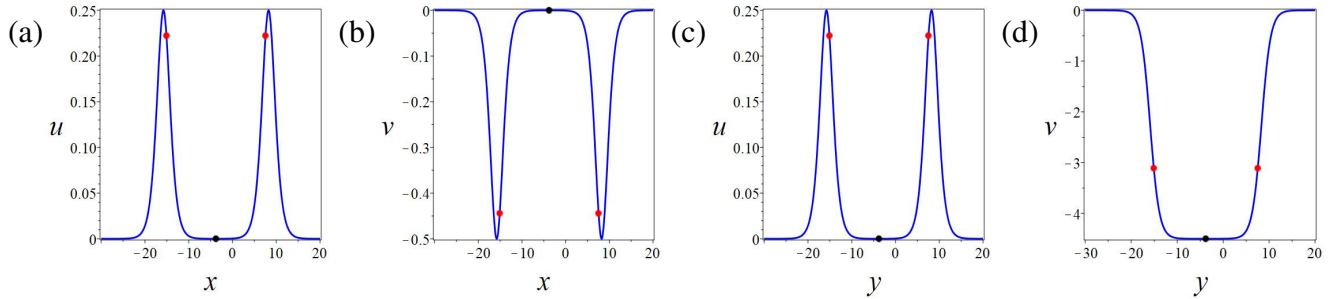


Figure 5: (a) (b) The cross-sectional curves (29) with parameters: $k_1 = 1, k_2 = -1 - \epsilon, p_1 = 1, p_2 = 2$; The black points are corresponding to P_2 , and the red points are corresponding to C and D . (c) (d) The cross-sectional curves (30) with parameters: $k_1 = 1, k_2 = 2, p_1 = 1, p_2 = -1 - 10^{-10}$.

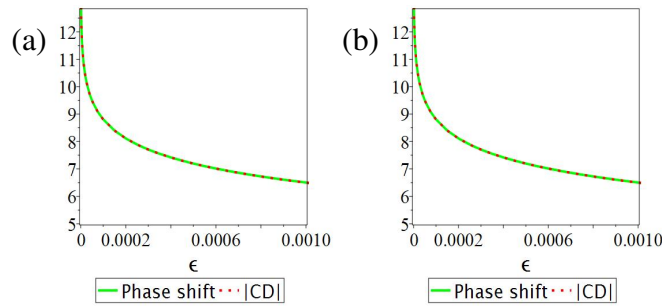


Figure 6: Parameters: (a) $k_1 = 1, k_2 = -1 - \epsilon, p_1 = 1, p_2 = 2$; (b) $k_1 = 1, k_2 = 2, p_1 = 1, p_2 = -1 - \epsilon$.

Fig. 5 illustrates the cross-sectional curves corresponding to Fig. 4. By taking the derivative of Eq. (29), we can determine their extreme values. Notably, as the same to S_{1-2} , the constant length stem S_{1+2}

exhibits only one extreme point between C and D . The coordinates of the extreme points of $u|_{\tilde{l}_{1+2}}$ and $v|_{\tilde{l}_{1+2}}$ in the (x, y) -direction are as follows:

$$P_2 : \left(\frac{(p_1 - p_2) \ln a_{12} + 2(k_1^3 p_2 - k_2^3 p_1)t + 2p_1 \xi_2^0 - 2p_2 \xi_1^0}{2(k_1 p_2 - k_2 p_1)}, -\frac{(k_1 - k_2) \ln a_{12} + 2(k_1^3 k_2 - k_1 k_2^3)t + 2k_1 \xi_2^0 - 2k_2 \xi_1^0}{2(k_1 p_2 - k_2 p_1)} \right) \quad (31)$$

Remarkably, P_2 precisely corresponds to the midpoint of CD , depicted as black dots in Fig. 5. Substituting (31) into (2) and (6) yields the extreme values as follows: $u(P_2) = -\frac{(k_1+k_2)(p_1+p_2)}{2} \sqrt{a_{12}} \approx -\frac{(k_1+k_2)(p_1+p_2)}{2}$ and $v(P_2) = -\frac{(k_1+k_2)^2}{2} \cdot \frac{(k_1+k_2)^2 \sqrt{a_{12}+(k_1-k_2)^2}}{(k_1+k_2)^2(\sqrt{a_{12}+1})} \approx -\frac{(k_1+k_2)^2}{2}$. These approximations further affirm the accuracy of the asymptotic forms (23). We can see again from Fig. 5 that the two ends of the stem are not the maximum or minimum points of u or v .

If we set $|k_1 + k_2| = \epsilon \approx 0$ or $|p_1 + p_2| = \epsilon \approx 0$ and $|k_j|, |p_j| \gg \epsilon$, we observe $|CD| \approx \Delta_{12}$. Fig. 6 visually represents how both “ $|CD|$ ” and “ $|\Delta_{12}|$ ” change with ϵ . Notably, when $\epsilon \approx 0$, the $|CD|$ curve closely aligns with the phase curve. Furthermore, the smaller ϵ is, the bigger $|CD|$ is.

5. Conclusions and discussions

Although soliton theory has been developed in several decades since 1960s, the essential properties of the stem structures is still not an unravelled problem. In this study, we have undertaken a systematic examination of localized stem structures in two solitons for the ANNV system. The constant length stem structures are consequences of quasi-resonant collisions between two solitons, exhibiting distinct characteristics of spatial locality and temporal invariance. Specifically, our investigation delineates two discernible scenarios: one characterized by $a_{12} \approx 0$ indicating a weakly quasi-resonant collision, and the other by $a_{12} \approx +\infty$ signifying a strongly quasi-resonant collision.

- Based on the asymptotic forms delineated in equations (9)–(11), comprehensive insights into the trajectories, amplitude, and velocity of each soliton arm have been extracted and cataloged in Table 1, along with the corresponding relationships encapsulated in equations (12) and (13). It is notable that the termini of the stem structure are rigorously defined as the points of intersection between l_1 and l_2 , as well as \tilde{l}_1 and \tilde{l}_2 . Concomitantly, the length of the stem S_{1-2} is explicitly formulated in Eq. (16). Moreover, the parametric description of the stem’s profile, articulated in equations (17) and (18), has been scrutinized to unveil its critical extreme points, illustrated in Fig. 2. This indicates that the extremal curve of the stem is not a horizontal line like a genuine soliton but rather a curve centered at the midpoint of the stem, gradually attenuating on both sides. By setting $|k_1 - k_2| = \epsilon \approx 0$ or $|p_1 - p_2| = \epsilon \approx 0$ with $|k_j|, |p_j| \gg \epsilon$, it becomes apparent that as ϵ approaches zero, the proximity between the $|AB|$ curve and the phase curve intensifies, connoting that diminishing ϵ values correspond to elongated stems.
- Similarly, drawing upon the asymptotic forms expounded in equations (21)–(23), an exhaustive analysis of the soliton arms’ trajectories, amplitudes, and velocities has been compiled in Table 1 and 2. Analogously, the terminal points of the stem structure are characterized as the intersections of l_1 with \tilde{l}_2 and \tilde{l}_1 with l_2 . Analogous to the previous scenario, the length of the stem, denoted as S_{1+2} , is methodically defined in Eq. (28). Furthermore, the mathematical representation of the stem’s profile, delineated in equations (29) and (30), has undergone meticulous scrutiny to identify its pivotal extreme points, depicted in Fig. 5. It further suggests that the extremal curve of the stem is a smooth curve centered at its midpoint. Analogous to the prior analysis, the reduction of $|k_1 + k_2|$ to $\epsilon \approx 0$ or $|p_1 + p_2|$ to $\epsilon \approx 0$, accompanied by $|k_j|, |p_j| \gg \epsilon$, demonstrates the convergent

alignment between the distance from $|CD|$ curve and the phase curve as ϵ tends to zero, signifying that diminishing ϵ values correspond to a lengthened stem structure.

A natural extension of our current work lies in the exploration of stem structures within higher order solitons. Beyond the quasi-resonant two-soliton case, the two-resonant three-soliton system can also give rise to localized structures, with the four surrounding branches interconnected by an intermediate soliton (stem structure) [41, 42]. In this phenomenon, the length of the stem gradually diminishes over time, leading to the fusion and subsequent separation of the surrounding soliton arms, while a new stem, oriented differently, reconnects them. This process, known as soliton reconnection, presents challenges in analyzing its local properties due to its complicated dynamic evolution over time. Future endeavors will focus on a comprehensive exploration of this phenomenon, aiming to provide deeper insights into the intricate dynamics of the ANNV system.

Conflict statement The authors declare that they have no conflict of interests.

Acknowledgments This work is supported by the National Natural Science Foundation of China (Grants 12071304 and 12201195), NUPTSF (Grants NY220161 and NY222169), the Natural Science Foundation of the Higher Education Institutions of Jiangsu Province (Grant 22KJB110004), Shenzhen Natural Science Fund (the Stable Support Plan Program) (Grant 20220809163103001), and Guangdong Basic and Applied Basic Research Foundation (Grant 2024A1515013106).

Reference

References

- [1] C. S. Gardner, J. M. Greene, M.D. Kruskal, R. M. Miura, Method for solving the Korteweg-de Vries equation, *Phys. Rev. Lett.* 19, 1095–1097 (1967)
- [2] F. Hagemann, and F. Hettlich, Application of the second domain derivative in inverse electromagnetic scattering, *Inverse Problems* 36, 125002 (2020)
- [3] V. B. Matveev and M. A. Salle, *Darboux Transformations and Solitons* (Springer-Verlag, Berlin, 1991)
- [4] C. H. Gu, H. S. Hu, Z. X. Zhou, *Darboux Transformations in Integrable Systems*, (Springer, Dordrecht, 2006)
- [5] J. S. He, L. Zhang, Y. Cheng, Y. S. Li, Determinant representation of Darboux transformation for the AKNS system, *Science in China Series A-Mathematics*, 49, 1867–1878 (2006)
- [6] J. S. He, H. R. Zhang, L. H. Wang, K. Porsezian, and A. S. Fokas, Generating mechanism for higher-order rogue waves, *Phys. Rev. E* 87, 052914 (2013)
- [7] R. Hirota, 2004 *The Direct Method in Soliton Theory* (Cambridge: Cambridge University Press)
- [8] B. K Berntson, E. Langmann and J. Lenells, On the non-chiral intermediate long wave equation: II. Periodic case, *Nonlinearity* 35, 4517–4548 (2022)
- [9] J. G. Rao, A. S. Fokas, J. S. He, Doubly Localized Two-Dimensional Rogue Waves in the Davey-Stewartson I Equation, *J. Nonlinear Sci.* 31, 67 (2021)
- [10] J. G. Rao, J. S. He, Y. Cheng, The Davey-Stewartson I equation: doubly localized two-dimensional rogue lumps on the background of homoclinic orbits or constant, *Lett. Math. Phys.* 112, 75 (2022).
- [11] N. Zabusky and M. Kruskal, Interaction of solitons in a collisionless plasma and the recurrence of initial states, *Phys. Rev. Lett.* 15, 240 (1965).

- [12] C. S. Gardner, J. M. Greene, M.D. Kruskal, R. M. Miura, Korteweg-deVries equation and generalizations VI: methods for exact solution. *Comm. Pure Appl. Math.* 27, 97–133 (1974)
- [13] M. J. Ablowitz and H. Segur, *Solitons and the Inverse Scattering Transform* (SIAM, Philadelphia, 1981)
- [14] M. J. Ablowitz, P. A. Clarkson, *Solitons: nonlinear evolution equations and inverse scattering*. (Cambridge University Press, Cambridge, 1991)
- [15] A. C. Newell, *Solitons in Mathematics and Physics* (Society for Industrial and Applied Mathematics, Philadelphia, 1985)
- [16] J. Miles, Resonantly interacting solitary waves, *J. Fluid Mech.* 79, 171–179 (1977).
- [17] H. Yeh, W. Li, and Y. Kodama, Mach reflection and KP solitons in shallow water, *Eur. Phys. J. Special Edition* 185, 97 (2010)
- [18] T. Maxworthy, On the formation of nonlinear internal waves from the gravitational collapse of mixed regions in two and three dimensions, *J. Fluid Mech.* 96 (1980), 47–64.
- [19] F. Kako, N. Yajima, Interaction of Ion-Acoustic Solitons in Two-Dimensional Space, *J. Phys. Soc. Japan* 49, 2063–2071 (1980)
- [20] K. Ohkuma and M. Wadati, The Kadomtsev-Petviashvili equation: the trace method and the soliton resonances, *J. Phys. Soc. Japan*, 52, 749–760 (1983)
- [21] M. J. Ablowitz and D. E. Baldwin, Nonlinear shallow ocean-wave soliton interactions on flat beaches, *Phys. Rev. E* 86, 036305 (2012)
- [22] M. Boiti, J. J. P. Leon, M. Manna and F. Pempinelli, On the spectral transform of a Korteweg-de Vries equation in two spatial dimensions, *Inverse Problems* 2, 271 (1986)
- [23] R. Hirota and J. Satsuma, N-soliton solutions of model equations for shallow water waves, *J. Phys. Soc. Japan.* 40, 611 (1976)
- [24] S. Y. Lou and X. B. Hu, Infinitely many Lax pairs and symmetry constraints of the KP equation, *J. Math. Phys.* 38, 6401 (1997)
- [25] P. A. Clarkson and E. L. Mansfield, On a shallow wave equation, *Nonlinearity* 7, 795 (1994)
- [26] P. G. Estévez and S. Leble, A wave equation in 2+1: painleve analysis and solutions, *Inverse Problems* 11, 925 (1995)
- [27] H. Y. Ruan and Y. X. Chen, Restudy of the structures and interactions of the soliton in the asymmetric Nizhnik-Novikov-Veselov equation, *J. Phys. A: Math. Gen.* 37, 2709 (2004)
- [28] H. C. Hu, X. Y. Tang, S. Y. Lou, Q. P. Liu, Variable separation solutions obtained from Darboux transformations for the asymmetric Nizhnik-Novikov-Veselov system, *Chaos Solitons Fractals* 22, 327 (2004)
- [29] E. Fan, Quasi-periodic waves and an asymptotic property for the asymmetrical Nizhnik-Novikov-Veselov equation, *J. Phys. A: Math. Theor.* 42, 095206 (2009)
- [30] A. M. Wazwaz, Structures of multiple soliton solutions of the generalized, asymmetric and modified Nizhnik-Novikov-Veselov equations, *Appl. Math. Comput.* 218, 11344–11349 (2012)
- [31] Z. Zhao, Y. Chen and B. Han, Lump soliton, mixed lump stripe and periodic lump solutions of a (2+1)-dimensional asymmetrical Nizhnik-Novikov-Veselov equation, *Mod. Phys. Lett. B* 31, 1750157 (2017)
- [32] J. G. Liu, Lump-type solutions and interaction solutions for the (2+1)-dimensional asymmetrical Nizhnik-Novikov-Veselov equation, *Eur. Phys. J. Plus* 134, 56 (2019)
- [33] J. Manafian, O. A. Ilhan, Ladan Avazpour, As'ad Alizadeh, N-lump and interaction solutions of localized waves to the (2+1)-dimensional asymmetrical Nizhnik-Novikov-Veselov equation arise

- from a model for an incompressible fluid, *Math. Meth. Appl. Sci.* 43, 9904–9927 (2020).
- [34] L. J. Guo, J. S. He, and D. Mihalache, Rational and semi-rational solutions to the asymmetric Nizhnik-Novikov-Veselov system, *J. Phys. A: Math. Theor.* 54, 095703 (2021)
 - [35] L. J. Guo, L. H. Wang, L. Chen, J. S. He, Dynamics of the rogue lump in the asymmetric Nizhnik-Novikov-Veselov system, *Stud. Appl. Math.* 151, 35–59 (2023)
 - [36] Z. L. Zhao and L. C. He, Resonance Y-type soliton and hybrid solutions of a (2+1)-dimensional asymmetrical Nizhnik-Novikov-Veselov equation, *Appl. Math. Lett.* 122, 107497 (2021)
 - [37] L. Jiang, X. Li and Biao Li, Resonant collisions among diverse solitary waves of the (2+1)-dimensional asymmetrical Nizhnik-Novikov-Veselov equation, *Phys. Scr.* 97, 115201 (2022)
 - [38] R. Radha, M. Lakshmanan, Singularity analysis and localized coherent structures in (2+1)-dimensional generalized Korteweg-de Vries equations, *J. Math. Phys.* 35, 4746–4756 (1994)
 - [39] Y. Matsuno, *Bilinear Transformation Method* (Academic, New York 1984)
 - [40] L. J. Guo, M. Zhu and J. S. He, Asymptotic analysis of the higher-order lump in the Davey-Stewartson I equation, *J. Math. Phys.* 64, 123505 (2023)
 - [41] K. Nishinari, K. Abe, and J. Satsuma, A new-type of soliton behavior in a two dimensional plasma system, *J. Phys. Soc. Jpn.* 62, 2021–2029 (1993)
 - [42] G. Biondini, D. Kireyev and K. Maruno, Soliton resonance and web structure in the Davey-Stewartson system, *J. Phys. A: Math. Theor.* 55, 305701 (2022)